Available online at www.sciencedirect.com
ScienceDirect
Thin Solid Films 515 (2006) 141 – 151
thin solid films
www.elsevier.com/locate/tsf

Al_2O_3 thin coating of AA 6082 T6 components using a fast regime fluidized bed

Massimiliano Barletta [a,*], Girolamo Costanza [a], Riccardo Polini [b]

[a] Dipartimento di Ingegneria Meccanica, Università di Roma Tor Vergata, Via del Politecnico 1, 00133 Rome, Italy
[b] Dipartimento di Scienze e Tecnologie Chimiche, Università di Roma Tor Vergata, Via della Ricerca Scientifica 1, 00133 Rome, Italy

Available online 18 January 2006

Abstract

Fluidized bed processing is a relatively novel method for coating metal substrates. A detailed study was carried out into surface property and in micro-structure changes induced by fluidized bed processing. In particular, fluidized bed processing of AA 6082 T6 aluminum alloy components using alumina Al_2O_3 powder was investigated. Firstly, the build up of Al_2O_3 films was studied and characterized in terms of coating thickness and adhesion. It was found that trends of deposited Al_2O_3 were consistent with fluidized bed processing time. Secondly, the effect of fluidized bed treatment on surface properties of processed components was examined. Surface morphology was significantly affected and its evolution according to processing time was accounted for. Both compressive residual stresses and increased dislocation density were induced by treatment of external layers of samples, and significant hardening was also detected. Lastly, the ability of fluidized bed processing was tested on 'ad hoc' fatigue samples. Rupture of fluidized bed treated samples as well as untreated samples was also discussed. At any rate, the fatigue behavior of processed components significantly improved. This quite new and unprecedented result is ascribed to the compressive residual stresses and work hardening induced by FB treatment in the outermost surface layers of the aluminum alloy.

Keywords: Fluidized bed; Al_2O_3 film; Fatigue

1. Introduction

In the research and development phase, highly stressed components such as turbine blades, connecting rods, and pistons demand optimum assessment of several aspects such as materials, manufacturing process, and design, with the actual choices being based on real world use and loading conditions. Consequently, the material surface plays a crucial role in all the components submitted to dynamic, or more specifically, vibrating loads because fatigue cracks usually start appearing in the surface where defects develop or alterations occur, such as notches, pores, fatigue slip steps, and inclusions [1]. However, the choice of a material for such special components as these can be very complicated. The most appropriate material should meet several requirements so that it supports the static and dynamic loading requirements, bears the critical demands in relation to phenomena of wear, erosion, and corrosion, as well as meet the need for easy manufacturing and processing [2]. A material able to fulfill all these demands does not currently exist. In most cases it can only be manufactured by material combination or a composite design with, to say the least, high costs and tricky operating procedures. In this respect, several industrial sectors are finding a variety of techniques for surface treatment ever more attractive as valid alternatives to design of high performance or special materials. Today three typical procedures are used to improve the untreated substrate material [3]: mechanical surface treatment, surface diffusion treatment, and surface overlay coatings.

In recent years, interest in techniques based on the application of surface overlay coatings onto the metal substrates has increased significantly. Indeed, the application of a quality coating on a substrate offers several returns, such as prolonged life time, improved hardness, high wear resistance, reduced friction, enhanced corrosion resistance, the establishment of a diffusion and oxidation barrier, as well as reduced maintenance loads and manufacturing costs [4]. In this field, Al_2O_3 films are the most widely used coatings in mechanics,

* Corresponding author.
E-mail address: barletta@mercurio.mec.uniroma2.it (M. Barletta).

0040-6090/$ - see front matter © 2005 Elsevier B.V. All rights reserved.
doi:10.1016/j.tsf.2005.12.093

microelectronics, and optics because of their special thermo-mechanical, chemical, electrical, and optical properties [5]. Several techniques are available to deposit Al_2O_3 films on Al substrates such as electrophoresis, physical and chemical vapor deposition, as well as high velocity and plasma spray process [3]. In improving the surface properties of processed parts such techniques can apply well-adherent films in the range of a few to hundreds of microns. Nevertheless, only limited effects of Al_2O_3 films on the fatigue behavior of coated parts can be expected, being connected to the improvement of surface morphology (reduction of surface roughness). In particular, this process cannot be expected to prevent dislocation movement in the surface layer of coated parts by either a local increase of the yield strength in the outer surface (mechanical hardening) or by introducing favorable compressive residual stresses. On the contrary, these effects are typically induced onto substrates processed by mechanical treatments, such as shot peening, even if they often concurrently cause a deterioration in aesthetic aspect and the finishing of exposed surface, as well as causing several problems connected with setting the most appropriate operating parameters, not to mention high plant, operating, and running costs [6–8].

To the knowledge of authors, no technique yet exists which can combine the typical advantages of coating process and mechanical treatments in a single process. In this context, a relatively novel 'hybrid' technique based on a fluidized bed of abrasive powders was proposed to simultaneously coat and mechanically treat the processed substrates so that the performance of both mechanical and coating techniques would be obtained using a single step process. In particular, this paper deals with the processing of AA 6082 T6 components based on a fast regime fluidized bed (FB) of Al_2O_3 powder. An assessment was made of the ability of this technique to coat processed parts with Al_2O_3 film in the range of few micrometers, thus improving their surface properties, and concurrently improving their fatigue behavior significantly. First, the build up of an Al_2O_3 film on aluminum slabs was discussed and film performance was estimated in terms of amount of Al_2O_3 deposited, film adhesion, surface morphology, and hardness. In addition, the improvement of surface properties of processed components was evaluated using X-Ray Diffraction (XRD). Next, the effect of FB processing on AA 6082 T6 fatigue behavior was assessed and rupture of untreated and FB-treated samples was examined. Lastly, some practical aspects concerning industrial employment of FB processing were also discussed.

Experimental findings showed that a tough and well-adherent Al_2O_3 film could be obtained using FB of Al_2O_3 powder. Such films were consistently found to grow in relation to FB processing time. Furthermore, FB processing was found to cause both the onset of compressive residual stresses and an increased hardening level in external layers on processed components without significant erosive phenomena on treated surface. This caused significant improvement in fatigue behavior of processed parts, which exhibited even greater fatigue endurance enhancements than one order of magnitude.

2. Experimental

2.1. Materials

AA 6082 T6 aluminum alloy was employed as substrate material for FB processing. This alloy was chosen because of the extensive commercial diffusion of such aluminum alloy and its surprising mechanical properties. Table 1 summarizes the material properties, and its typical composition is reported in Table 2. Three types of specimens were investigated. Two types of slabs were cut from 6 m long bar, measuring $100 \times 10 \times 25$ mm and $10 \times 10 \times 5$ mm. The closest geometrical tolerances (<0.05 mm) and uniform starting surface condition were assured by thorough controls. From a 6 m long rod, 120 mm long and 16 mm diameter fatigue test samples with a test zone 7 mm in length and 8 mm as diameter were made by high speed turning. A very special tool was used to machine the test zone of the fatigue samples in order to guarantee the best surface finish and to minimize the risk of surface defects or alterations. All the materials employed in this experimental campaign came from the same foundry so that reproducible behavior would be ensured.

Alumina Al_2O_3 powder (supplied by Smyris Abrasivi Srl, Italy) with a mesh size of 16 and shape factor of 0.67 was used as abrasive media for FB processing. The most important properties of the Al_2O_3 powder used are reported in Table 1. Before being employed in the FB, the alumina powders were preventively sieved using a standard 120 mesh size in order to remove all the fines. After this, a maximum working time of 4 h was allowed for sieved alumina powder in FB processing. Finally, the worn out alumina powder was removed and fresh powders were provided.

2.2. Fluidized bed (FB) apparatus

The experimental fluidized bed (FB) apparatus is shown in Fig. 1 [9,10]. It processed the aluminum alloy components using alumina powders as 'media'. The fluidized bed consists of a vertical column, 200 mm square in cross-section and about

Table 1
Properties of Aluminum AA 6082 T6 and Alumina 98%

Mechanical properties	Material	
	Aluminum AA 6082 T6	Alumina 98%
Density, g/cm^3	2.7	3.8
Water absorption, %	–	0%
Hardness, Mohs	–	9
Hardness, Vickers	95	–
Tensile strength, ultimate MPa	300	200
Tensile strength, yield MPa	255	–
Elongation at break, %	10	–
Modulus of elasticity, GPa	69	300
Shear strength, MPa	200	–
Flexural strength, MPa	–	320
Compressive yield strength, MPa	–	2400
Poisson's ratio	–	0.22
Fracture toughness, MPa x m^{½}	–	4.5
Shear modulus, GPa	26	130

Table 2
Chemical composition of Aluminum AA 6082

Aluminum AA 6082 T6 composition	
Element	% wt.
Al	95.2–98.3
Mg	0.6–1.2
Si	0.7–1.3
Cr	≤0.25
Mn	0.4–1.0
Fe	≤0.5
Cu	≤0.1
Other	≤0.15

1600 mm high, together with a porous plate distributor. The column was made from stainless steel, with a thickness of 5 mm to provide wall rigidity and resistance to wear. It was provided with glass windows so that the fluidization process would be visible during the process. The porous plate distributor was made from a 3 mm thick stainless steel mesh. It was hosted just beneath the fluidization column, and it is used to support the alumina powder when it are not suspended, simultaneously ensuring vertical permeability to the incoming air flux when the fluidized bed is switched on. An obvious condition for the porous plate distributor to work properly is that it does not modify the velocity distribution imposed by the inlet section [9]. A Mapro model Turbotron blower with a maximum power of 37 kW was used to feed purified air flux free from oil and moisture into the inlet section of fluidized bed under strictly monitored process conditions. In fact, a standard flowmeter with a 24 V output and an Mitsubishi inverter model FR-A-540-30k were respectively used to read the current value of air flux and correct it so that the flow rate was kept constant throughout the treatment. A pressure probe, a hygrometer, and a thermocouple set were also used to monitor the process and to assure environmental conditions were kept constant, thereby guaranteeing the best reproducibility of experimental settings.

2.3. Experimental procedure

Al_2O_3 powder was used as fluidizing material with a static bed height of 200 mm. Fluidization of Al_2O_3 powder is observed when the 'fixed' bed comes in contact with a vertical upward fluid, in an intermediate range of flow rates. The air flux suspends the powder, increasing its volume, and makes the powder act like a liquid. Each particle becomes individually suspended in the fluid flow, while on the whole the bed remains motionless relative to the column walls; the bed is said to be fluidized. A minimum fluidization velocity of about 0.25 m/s was calculated for the Al_2O_3 powder employed. Each time the fluidized bed was loaded with fresh alumina powder, it was run for a few minutes at low flow rates (<200 m^3/h) in order to ensure thorough mixing of powder. After that, flow rates as high as 650 m^3/h were set to activate the fluidization regime to perform sample treatment. Treatment times ranging from 15 min to 4 h were chosen.

During FB processing all the slabs were simply clamped from the top as shown in Fig. 1, and in a fixed position dipped in the dense phase of the FB (230 mm away from the porous plate distributor). They were then submitted to repeated strikes from abrasive grains driven by the fluid onto the exposed surface. Half one side of each sample was protected by a thick rubber masking in order to attain both an FB-treated and an untreated zone on the same surface, thus allowing straight comparison of the two. On the contrary, fatigue samples were clamped on the shaft of a direct current electric motor and rotated at 100 Hz during FB treatment in order to assure process uniformity over the entire sample surface. A system composed of a digital revolving counter provided with a 24 V output and an inverter was used to monitor the rotating speed of the fatigue samples and to keep it constant throughout the FB processing.

However, being the fluidized bed able to confer the transport properties of a fluid to the mix of air and Al_2O_3

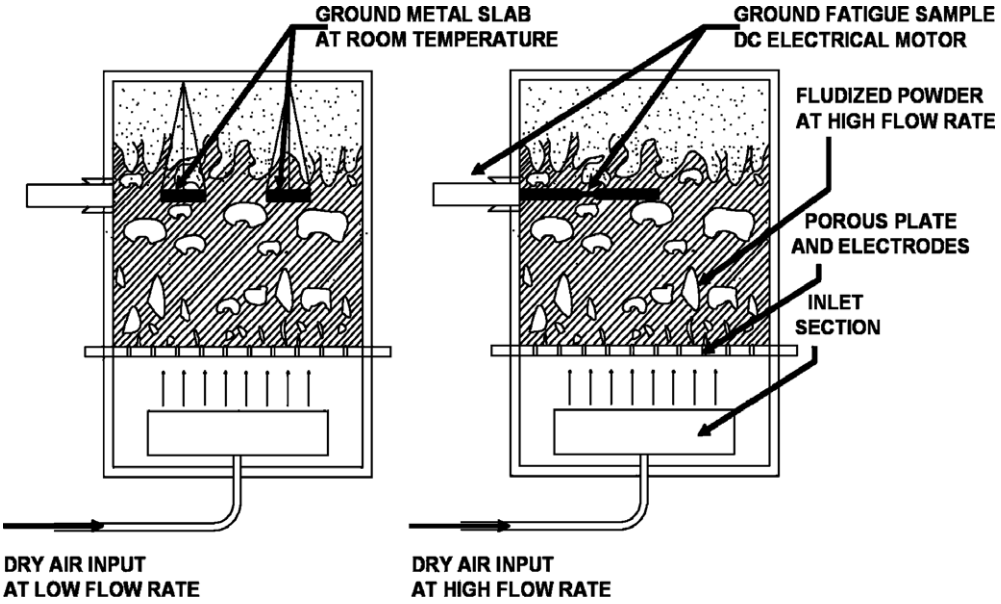

Fig. 1. Fluidized bed apparatus and sample location during fluidized bed processing.

powder [9], the best uniformity of the treatment can be attended all over the surface of exposed samples.

2.4. Characterization tests

The effects of FB processing were measured by calculating the amount of alumina deposited above the sample surface. Small $10 \times 10 \times 5$ mm slabs were used so that even the slightest variation in sample weight could be measured. The small slabs were carefully cleaned before and after exposure to the abrasive media. Since the mass of deposited alumina was very small, the employment of a very accurate and reliable measurement technique was of fundamental importance. Digital scales (Sartorious Model BP 211-D) with a readability of 0.01 mg were used. To minimize any disturbances, the scales were enclosed in a box to prevent air currents. Two special aluminum slabs were kept separately and used as standard weights to calibrate the scales each time they were used. These special efforts allowed the scales to perform the measurements to the required accuracy, and with good reproducibility. To avoid getting both dust and oxides on slab surfaces, they were removed from the FB immediately after being processed. The weight of the starting slabs was taken with particular caution. Then after the test, a very fine tissue (Kimwipes®) was used to clean the sample surface. Following this, the samples were put into a dryer. A further passage with the tissue was performed and the slab was weighed as soon as possible afterwards. In carrying out the measurements the scales were left until the digital display of the results shown on the scales stabilized. Each sample was measured several times and, if the difference between the two following measurements failed to agree within 0.05 mg, the measurements were repeated until agreement within this range was attained in successive determinations. To monitor the wear of the metal specimens, a 1 μm resolution digital palmer Mitutoyo Digimatic model was used. To take into account the evolution of surface morphology of processed samples, surface roughness measurements were performed with a Taylor-Hobson instrument model Form Talysurf Intra, and TalyMap software was used to process the experimental data.

After FB processing, the larger slabs ($100 \times 40 \times 25$ mm) were characterized by Field Emission Scanning Electron Microscopy (FE-SEM, Leo Supra 35) and Energy Dispersive X-Ray Spectroscopy (EDS, Oxford Instruments Ltd., Inca 300 model) to study the build up of the Al_2O_3 film. After this, the slabs were submitted to XRD analysis to investigate the changes in surface properties induced by FB treatment, comparing the treated and untreated zone of each sample. A Philips model X'Pert Pro was used as diffractometer type, with a generator voltage set at 40 kV and a tube current set at 40 mA. Cu Kα radiation ($\lambda = 1.54$ Å, graphite filtered) was used. Adhesion tests were also performed by indenting the coated samples using both a spherical tip indenter (1/16″ diameter and made from stainless steel) and a Brale conical tip indenter (1/16″ diameter and made from mono-crystalline diamond) under variable load in the range of 5 to 150 kg. Microhardness tests were also performed using a micro Vickers indenter and applied loads in the range of 25 to 1000 g were employed for a duration of 10 s. Finally, a scratch test according to ASTM standard was performed using a cross hatcher provided with five parallel blades able to produce cutting into the substrate to a depth of 1.5 mm. To scan the surface conditions and evaluate the eventual delamination of film after indentation, hardness and scratch test, a Leica DM IRM model optical microscope was used at magnifications in the range of 50 to 200 X. In particular, the extended focus feature of the optical microscope was applied to catch the surface morphology of processed substrates at different altitudes. Then, the Leica MW composition image software was used to rebuild the 3D image so as to obtain the best focus condition at the various working distances.

2.5. Fatigue tests

Fatigue tests were performed to investigate the effect of FB process ('as received', mirror polished and 4 h FB-treated samples were compared), the influence of loading conditions ('as received' and 4 h FB-treated samples were compared), and FB processing time (untreated, 15, 60 and 240 min FB-treated samples were compared). All the fatigue trials were carried out using a rotating bending machine, single-end cantilever ($R = -1$, $n = 17$ Hz), and variable loads from 16 to 26 kg were applied, corresponding to a variable maximum amplitude of alternating stress (σ_{MAX}) in the range of approximately 150 to 230 MPa. After the rupture of fatigue samples, their cross-sections were thoroughly examined by using a Nikon SMZ-U Stereoscope and SEM (Leica Cambridge model 360).

3. Results and discussion

3.1. Fluidized bed (FB) processing: build up of Al_2O_3 film

The impact of the brittle Al_2O_3 powders on aluminum samples during FB treatment caused their splinter fragmentation and subsequent embedding of Al_2O_3 debris in the metal surface. Consequently, thin rapidly growing Al_2O_3 coating resulted. Fig. 2 reports an image of the inferred mechanism with the two types of impact: the sliding, typical of high impact speed and angle; and the rolling, typical of low impact speed or angle [11,12]. Both mechanisms caused the release of a very small part of incoming Al_2O_3 powder, which got stuck in the outermost layers of softer aluminum alloy, giving rise to the build up of the Al_2O_3 film onto it.

Fig. 3 shows SEM images of FB-coated aluminum slabs according to processing time. A progressively denser and more compact coating built up on the aluminum alloy substrate when longer FB processing time was applied. However, after processing for 15 min, there were still uncoated zones on the aluminum substrate. Fig. 4 shows an SEM image of coated and uncoated zones, and the corresponding EDS microanalyses are reported in Fig. 5. At least 60 min were necessary to completely cover the aluminum alloy substrate with a compact and uniform Al_2O_3 film. However, Fig. 6 reports a cross-section view of Al_2O_3 coating after 4 h processing. Al_2O_3

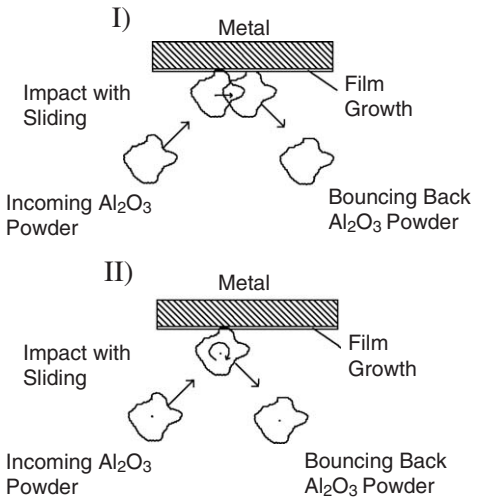

Fig. 2. Interaction between Al_2O_3 powder and aluminum substrate during fluidized bed processing.

coating was found to completely and uniformly cover all sample surface. A thin layer (about 10 μm) of Al_2O_3 was progressively deposited during the FB processing.

No significant wear phenomena were associated with FB processing. Differences in substrates thickness smaller than 3 μm did systematically show on the digital palmer, a value close to the resolution of the instrument and, in any case, within its limits of accuracy.

Fig. 7 reports the trend in mass growth according to FB processing time. Fast Al_2O_3 deposition was exhibited by the metal substrate during the first few minutes of FB treatment. As processing time elapsed, a sort of asymptotic level of Al_2O_3 deposition was reached after 60 min. In fact, if the substrates were exposed to longer FB treatment, only a slight increase in mass growth occurred. A hypothesis can be formed inferring progressive saturation of external layers of aluminum substrate due to the embedding of Al_2O_3 splinters into it. In fact, during

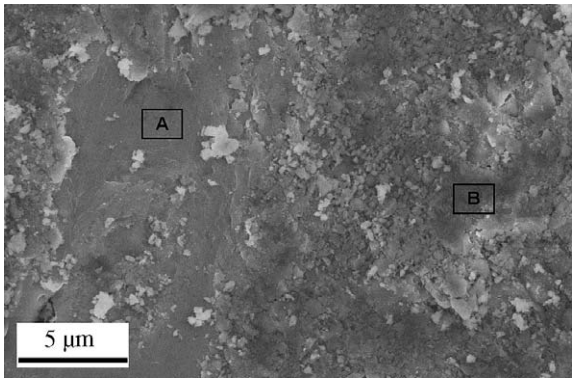

Fig. 4. SEM image of Al_2O_3 coatings after 15 min: uncoated (A) and coated zone (B).

the first part of FB treatment, the aluminum substrate was directly exposed to the abrasive action of Al_2O_3 grains. Al_2O_3 powders being much harder than aluminum substrate, and as they were projected at high speeds (in the range of 1 to 4 m/s) towards the substrate, a very fast build up of the Al_2O_3 film was obtained. Nevertheless, continuing towards higher processing time, when impacting onto substrate, the Al_2O_3 powders met a surface with deeply changed characteristics. In fact, the previously deposited Al_2O_3 film formed some sort of barrier to further deposition of Al_2O_3 splinters, as this coating is considerably harder than the starting aluminum substrate. Consequently, the deposition process slowed down. Next, continuing on to very high FB processing time (longer than 2–3 h), the increase in deposited alumina could be disregarded and the previously deposited Al_2O_3 film seems to have some sort of self-limiting effect on the growth of a thicker coating.

This mechanism has been confirmed by analyzing the chemical composition along the Al_2O_3 film after 4 h of FB processing. The quantitative EDS analyses of cross-sections of the Al_2O_3 film at various depths are reported in Table 3. As can be seen, moving away from the exposed surface, a coating

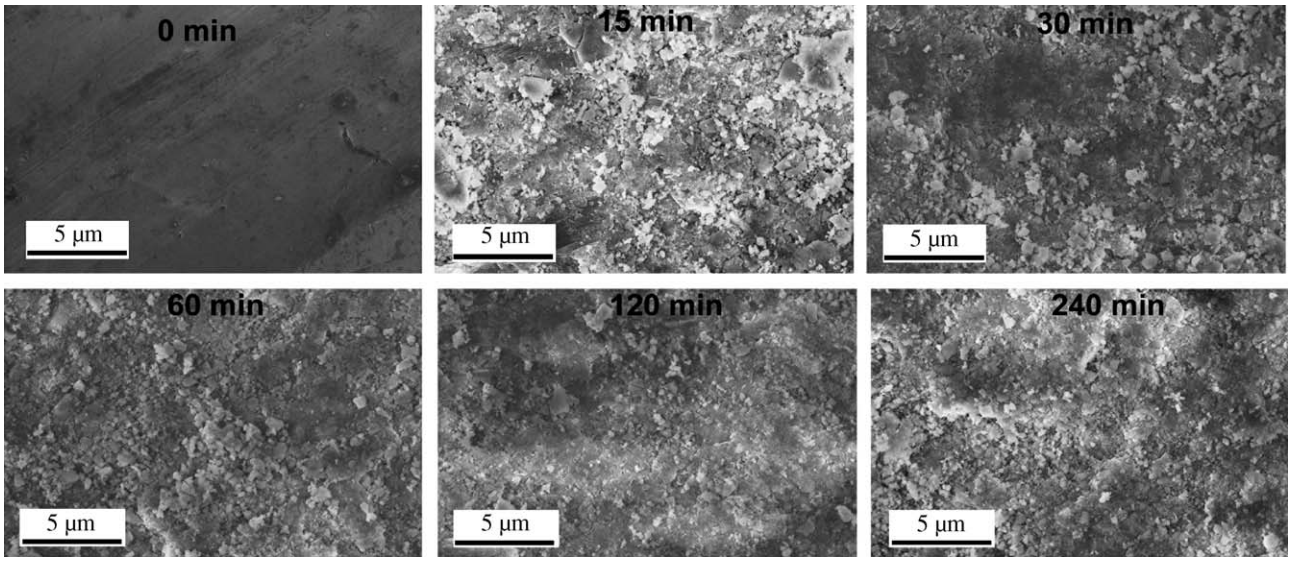

Fig. 3. SEM images of Al_2O_3 coatings on aluminum alloy according to fluidized bed processing time.

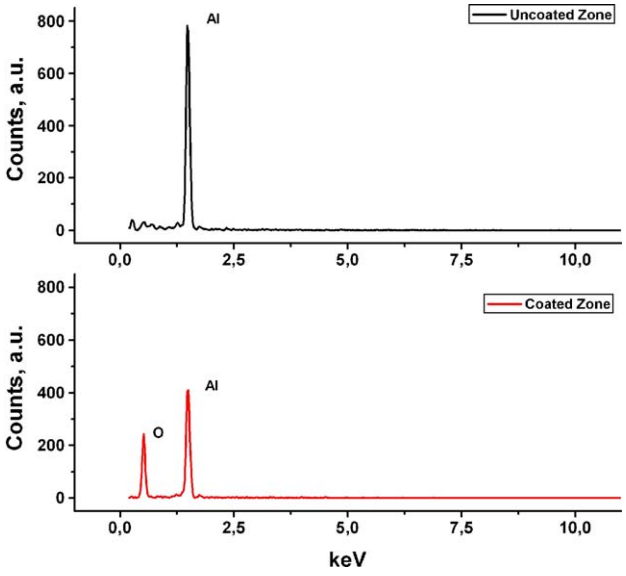

Fig. 5. EDS microanalysis of Al_2O_3 coatings after 15 min: uncoated (A) and coated zone (B).

thickness richer in aluminum and poorer in oxygen was detected. These findings confirm that the Al_2O_3 coating grew as a result of subsequent superimposition of embedded layers. The early layers deposited were richer in aluminum and constituted a kind of metal matrix composite (MMC). The layers deposited later were richer in oxygen and exhibited almost the same composition as starting Al_2O_3 powder.

3.2. Adhesion tests on Al_2O_3 film

Rockwell indentation test results revealed good adhesion of Al_2O_3 film on substrates, showing the increased resistance to penetration exhibited by FB-treated samples compared to untreated samples. Indentation loads in the range of 5 to 150 kg applied using both spherical and conical indenter did not produce delamination of the Al_2O_3 coating in all conditions investigated. The Al_2O_3 film was found to follow the plastic deformation of aluminum substrate under the indenter pressure, and no cracks occurred in substrates treated 4 h into FB (Fig. 8). Hence, in contrast to findings for different deposition techniques [3], the Al_2O_3 films did not exhibit brittle behavior.

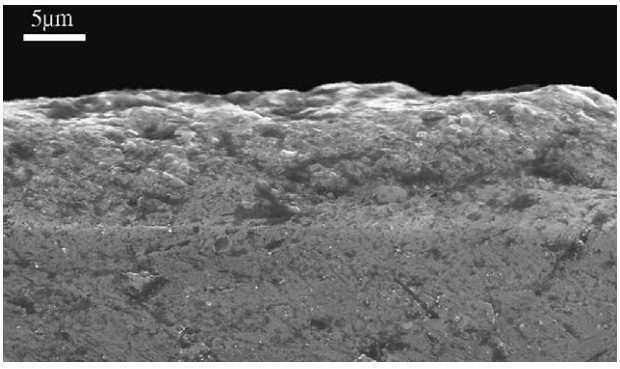

Fig. 6. SEM cross-section of Al_2O_3 coating on aluminum alloy.

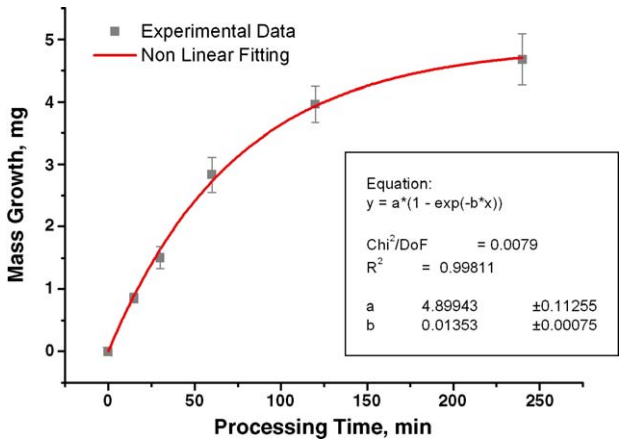

Fig. 7. Al_2O_3 mass growth trend according to fluidized bed processing time.

Since the pressure applied was as much as 500 MPa for the largest applied load, Al_2O_3 coatings deposited by FB definitely possess outstanding adhesion properties.

The results of the scratch test performed upon similarly treated substrates (4 h-treatment inside the FB) confirmed the previous experimental findings. Neither film delamination nor cracks occurred, and cracks were not propagated from the scratched area (Fig. 9).

3.3. XRD analysis of fluidized bed (FB) processed substrates

XRD analysis performed on FB-treated and untreated flat samples (Fig. 10) showed the modification of 6082 aluminum alloy diffraction peaks, and the appearance of Al_2O_3 peaks after FB treatment. Fig. 11 shows the low-angle shift of the Al(311) reflection for 1 and 4 h FB-treated samples, respectively. Fig. 11 also shows the broadening of the half-width diffraction peaks. Therefore, both the presence of compressive residual stresses and increased level of hardening of external layers of FB-treated samples can be seen.

An interpretation of both the previous considerations can be usefully provided. As said, our XRD tests ensure that compressive residual stresses are introduced in the external layer of the FB treated zone, since a low shift angle of XRD diffraction peak is observed (Fig. 11). This statement is

Table 3
EDS microanalysis along the cross-section of 4 h FB treated aluminum substrate

Composition, % wt. element	Depth under sample surface [μm]					
	0	3	6	9	12	100
Al	55.7	56.5	59.7	63.1	82.3	98.2
Cr	0	0	0	0	0	0
Cu	0	0	0	0	0	0
Fe	0	0	0	0	0	0
Mg	0.2	0,2	0,1	0,2	0,4	1,1
Mn	0	0	0	0	0.2	0.7
O	42.6	42	39.2	35.8	17	0
Other	1.5	1.3	1	0.9	0.1	0

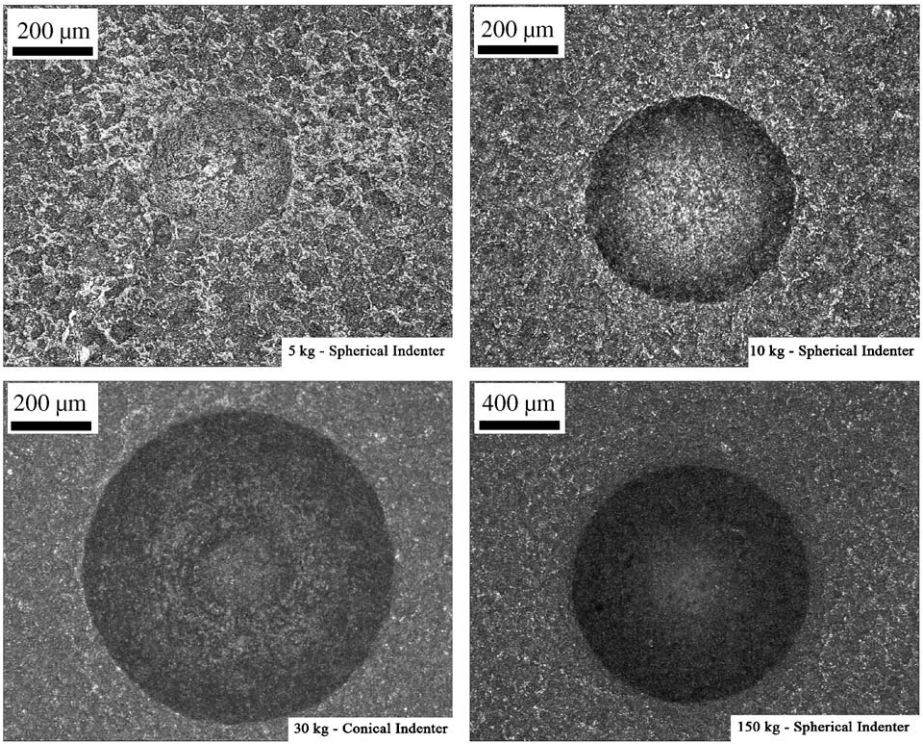

Fig. 8. Adhesion test of Al_2O_3 coating on aluminum alloy after 4 h fluidized bed processing time under Rockwell spherical indenter.

supported by the following theoretical considerations. The Bragg's law is as follows:

$$n\lambda = 2d\sin\theta \tag{1}$$

Rearranging it:

$$\frac{n\lambda}{2\sin\theta} = d \tag{2}$$

where d is the inter-planar distance of lattice.

The strain ε_{hkl} of a generic family of planes $\{hkl\}$ is given by:

$$\varepsilon_{hkl} = \frac{d_{FB} - d}{d_{FB}} \tag{3}$$

where d and d_{FB} are the inter-planar distance of untreated and FB treated substrates, respectively.

Since FB treatment determines a low angle shift of diffraction peak (Fig. 11), that is, a lowering of θ and, concurrently, of sin θ, d_{FB} is bigger than d and, consequently, ε_{hkl} is positive.

For an elastic, isotropic and homogenous solid, submitted to a tri-axial normal stress σ_x, σ_y and σ_z along the main axes x, y

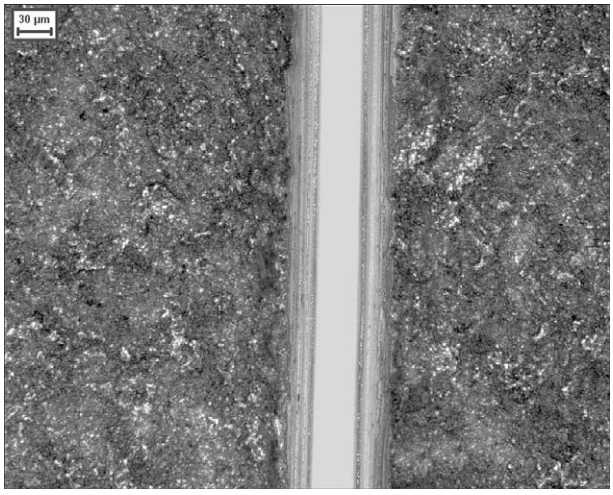

Fig. 9. Scratch test of Al_2O_3 coating on aluminum alloy after 4 h fluidized bed processing time.

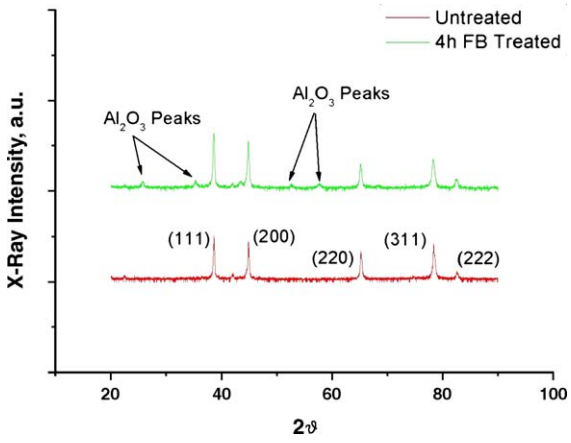

Fig. 10. Diffraction peak of fluidized bed treated and untreated substrate: the appearance of alumina peaks.

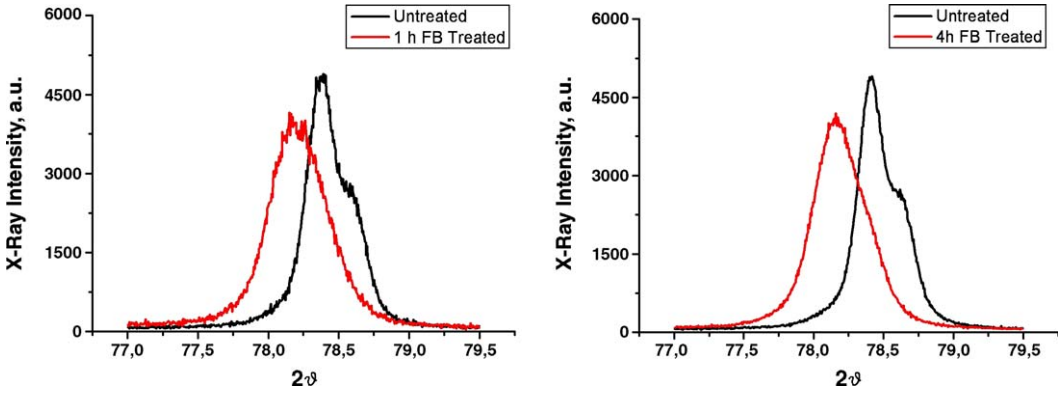

Fig. 11. Diffraction peak of fluidized bed treated and untreated substrate: low angle shift and peak broadening.

and z, the theory of elasticity predicts that the strain along z-axis is worth:

$$\varepsilon_z = \frac{1}{E}\left(\sigma_z - v\left(\sigma_x + \sigma_y\right)\right) \tag{4}$$

where E is the elastic modulus And v the Poisson's coefficient. If an hypothesis of bi-axial stress is formed, $\sigma_z=0$ and Eq. (4) can be rearranged:

$$\varepsilon_z = \frac{-v}{E}\left(\sigma_x + \sigma_Y\right) \tag{5}$$

Therefore, ε_z, that is, the strain measured with our XRD analysis, is due to stresses which act in the x–y plane. In our case, $\varepsilon_z=\varepsilon_{hkl}$ was found to be positive, hence the term $(\sigma_x+\sigma_Y)$ is negative. This means that the stress is compressive in x–y plane. As a consequence, even if specific measures of residual stresses were not performed, this result allows to explain, at least qualitatively, the different behaviour of FB treated and untreated aluminium alloy, with the birth of compressive residual stresses onto FB treated substrates.

Dislocation density was estimated. In particular, the experimental full width at half maximum, β_S, of the {311} reflection was corrected for the instrumental broadening β_E:

$$\beta_T = \beta_S - \beta_E \tag{6}$$

Depending only on micro-structural features of the material, β_T can be expressed as:

$$\beta_T = \beta_D + \beta_\varepsilon = \lambda/(D\cos\theta) + 2\varepsilon\tan\theta \tag{7}$$

where β_D and β_ε are the contributions to peak broadening due to size D of coherently diffracting domains and to the microstrain? ε, which is induced by defective structures and especially by dislocations. λ is the Cu Kα radiation wavelength. Since the mean grain size is larger than 30 μm, the initial contribution is negligible. The microstrain ε was determined from β_T. The density of dislocations (ρ) was determined using the relationship proposed by Williamson–Smallman [13]:

$$\rho = K\varepsilon^2/\left(k_0 b^2\right) \tag{8}$$

In Eq. (8) K (≈16) is a parameter connected with microstrain distribution, θ is the Bragg angle, b is the modulus of Burger's vector (2.86 Å for Al), and k_0 (≈1) is a factor that depends on the dislocation interaction. After 1 h treatment, the dislocation density increased by one order of magnitude (Table 4). As reported in Table 4 and as can be expected from the thickening of Al_2O_3 film, the dislocation density remained substantially unchanged for longer processing time.

Vickers micro-hardness tests confirmed the beneficial effect of FB processing on substrate properties, hence revealing the huge increment of surface hardness. Table 5 summarizes the differences in micro-hardness for untreated and 4 h FB-treated substrates under different loading conditions. Hardness values up to three times higher were detected for FB-treated surface. The largest differences arose for low loads, where the influence of the tough and well-adherent Al_2O_3 coating was very strong, the indenter only being able to penetrate into the first few layers of the substrate, thereby not going through the Al_2O_3 coating. With larger loads, the improvement in hardness values for FB-treated substrates remained very high, but the effect of the Al_2O_3 coating became progressively fainter, the indenter was able to penetrate deeply into material, going through the Al_2O_3 coating and touching also the aluminum substrate.

These findings could be ascribed to the massive increase of the dislocation density induced by plastic deformation of the substrate during FB processing. It was found that besides coating the aluminum substrates with an Al_2O_3 film, FB

Table 4
Dislocation density calculated using Eq. (3) from XRD

	As received	1 h FB-treated	4 h FB-treated
Dislocation density (cm^{-2})	2.58×10^{10}	2.12×10^{11}	1.88×10^{11}

Table 5
Vickers micro-hardness test for untreated and FB treated samples under different loading conditions

Hardness, HV	Same typology		Ratio
Load, g	As received	Fluidized bed	
50	91,5	N.D.	
100	90,3	243,7	2,70
200	88,7	186,7	2,10
500	89,3	146,3	1,64
1000	86,2	122,2	1,42

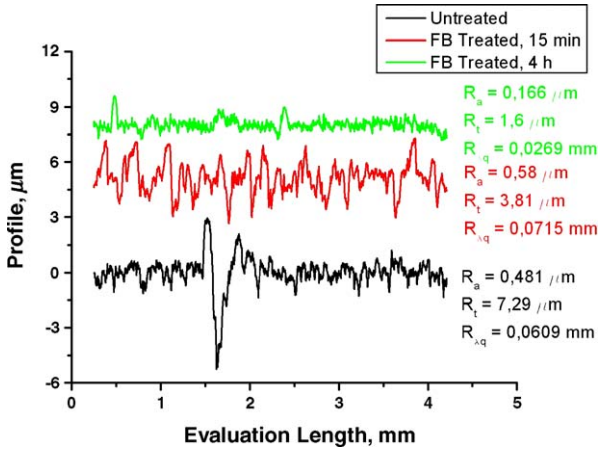

Fig. 12. Roughness profile of untreated, 15 min fluidized bed treated and 4 h fluidized bed treated substrate.

processing also mechanically treat the substrates, hence changing both the XRD spectrum and the micro-hardness values of processed material. A very similar mechanism to that typical for mechanical treatment (i.e., shot peening [1]) can therefore be inferred: upon the repeated impacts of Al_2O_3 powder, widespread micro-craters are generated over the entire exposed surface. The processed material was locally stressed during repeated impacts far above its yield strength so that plastic flow occurs locally with the formation of a micro-hill and micro-valley topography (see 15 min FB-treated profile in Fig. 12). In the early stages of Al_2O_3 powder micro-impacts, tensile stresses were probably produced at the sample surface since the surface may become plastically larger which agrees with what typically happens on shot-peened surface [14,15]. As a reaction to the repeated impacts, compressive residual stresses were formed in the outermost surface layers, being balanced by residual tensile stresses in the elastically deformed component interior.

While proceeding toward higher FB processing time, a progressive improvement of surface morphology was also detected (see 4 h FB-treated profile in Fig. 12). In fact, the deposition of the Al_2O_3 film onto the substrate may well cover the micro-hill and micro-valley topography generated by the FB processing of the aluminum substrate, thus reducing the average roughness (up to 0.166 μm) and the slope parameter (up to 0.0269 mm). Furthermore, the finishing ability of FB makes it an even more promising specialized surface treatment technique compared to other mechanical treatments technologies like shot peening. In fact, the main risk of shot peening is the over-peening of exposed surface, which is typically due to incorrect settings of operative parameters [1]. This produces considerable deterioration of surface finishing, which influences fatigue behavior [16,17] and the overall performance of exposed surface negatively. Besides, shot peening is a high pressure process with several drawbacks related to plant and running costs, automation and control procedure, operators' safety, and environmental impact [7]. On the contrary, FB processing being a very low pressure process, can be operated and controlled using basic equipment, has low running costs, and does not require any specific precautions for operators safety, nor to avoid environmental impacts [9]. Furthermore, it can be scaled-up and completely automated without tricky or expensive procedures [10].

Table 6
Fatigue tests for as received samples and FB-treated samples under different loading conditions: number of fatigue cycle to rupture, N_f

Load, kg	Stress, MPa	N_f, untreated	Load, kg	Stress, MPa	N_f, FB treated
17	149,2	5,40E+06	19	166,7	6,51E+06
18,5	162,3	1,76E+06	20	175,5	3,24E+06
20	175,5	6,75E+05	22	193,1	1,94E+06
22	193,1	1,60E+05	26	228,2	3,60E+05

Table 7
Fatigue tests for as received samples, as mirror polished samples and FB treated samples: number of fatigue cycle to rupture, N_f

N_f	Sample typology		
Load, kg	As received	Mirror polished	Fluidized bed
20	6,75 E+05	5,2 E05	4,68 E+06

3.4. The fatigue behavior of processed substrates

Findings in previous experiments are very promising. All treatments that should mechanically improve the fatigue strength of components are based on the principle of preventing dislocation movement in the surface layer by either local increase of the yield strength in the outer surface (mechanical hardening) or by the introduction of favorable compressive residual stresses. In addition, it is well known that improvements to component fatigue strength can result from better surface finishing.

Accordingly, fatigue tests showed significant improvement in the fatigue behavior of FB-treated samples compared to untreated samples (Table 6). According to experimental results, the increment of the number of cycles to fracture was remarkable in all investigated conditions. There is a 7 to 12 times increase compared to 'as received' samples under the same loading condition (20 and 22 kg, respectively). Such improvements are attributable to the compressive stresses, the increased level of hardening, and the good surface finishing found on the surface, which retard crack nucleation, thereby improving fatigue behavior. If the averaged number of cycles to fracture of FB-treated and 'mirror polished' samples is compared, an improvement of more than 20 times is found under applied load of 20 kg (Table 7). Besides, surprisingly, the 'as received' samples were found to behave better than the 'mirror polished' samples. This was probably due to an introduction of favorable residual stresses as well as to an

Table 8
Fatigue tests varying processing time for FB treated samples: number of fatigue cycle to rupture, N_f

N_f	Processing time, min			
Load, kg	0 min	15 min	60 min	240 min
22	1,60E+05	4,24E+05	1,51E+06	1,94E+06

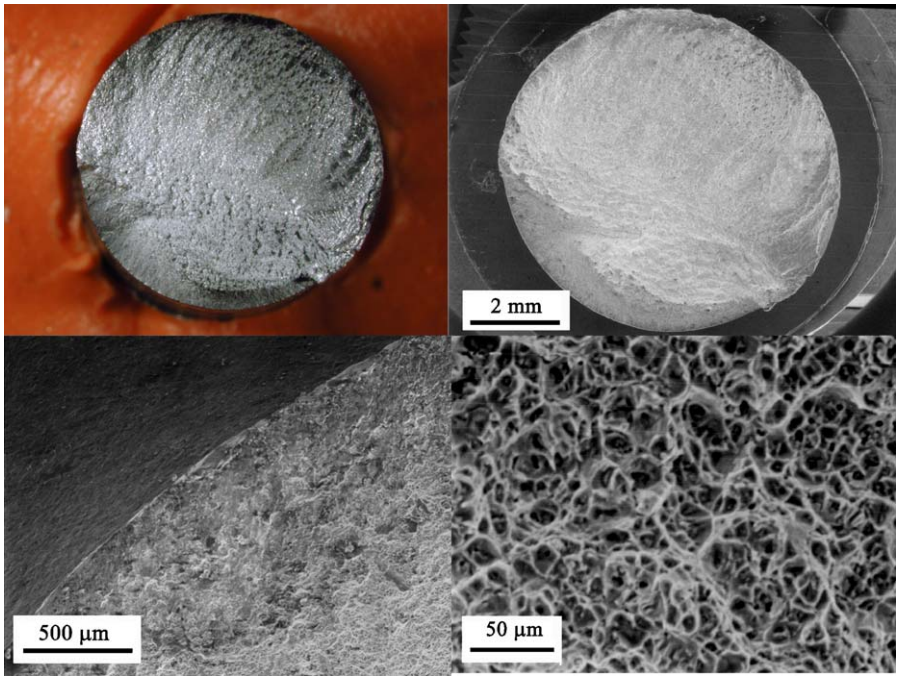

Fig. 13. Stereoscopy and SEM images of fatigue sample cross-section after rupture: 4 h fluidized bed treatment.

increased hardening level induced on the 'as received' samples by high speed turning in agreement with experimental findings reported in the relevant literature [18,19]. Regarding the influence of processing time on fatigue behavior of FB treated samples (Table 8), it was estimated that after 15 min fatigue behavior improved 3 to 4 times. In addition, after 1 h the number of cycles to fatigue rupture was approximately 80% of the maximum values measured after 4 h of FB processing. This agrees with the 'saturation effect' hypothesis for Al_2O_3 deposition (Fig. 7), and with results from XRD analysis which showed similar behavior between 1 h and 4 h FB treated samples (Fig. 11).

Fig. 13 shows the rupture process in FB-treated samples. All the samples exhibited superficial cracks, which initially propagated parallel to the rotation axis of the sample towards the area subjected to lower stress during fatigue test, remaining to one side of it. After that, a ductile rupture of the sample occurred, starting on the side of crack nucleation and growing toward the opposite side. SEM analyses of the fractured surface revealed no differences in the way FB-treated and untreated samples fractured. Furthermore, no differences in the rupture process or anomalies are exhibited by 'as received' and 'mirror polished' samples. Cracks propagate slowly during the first part of fatigue life (low ΔK values), and the surface appears to be smooth due to rubbing. Crack growth accelerates in the final part of fatigue life (high ΔK values) and the dimples show the evident ductile rupture process in the plastic zone.

4. Conclusions

This paper presents a detailed study of the effect of a fast regime fluidized bed of Al_2O_3 powder onto high-strength aluminum alloy, with particular attention being paid to Al_2O_3 coating build up and the fatigue behavior of processed substrates.

Fluidized bed process was found to coat aluminum alloy substrates with a tough and well-adherent Al_2O_3 coating. The good adhesion of Al_2O_3 coatings onto aluminum substrates was seen in both Rockwell indentation under different loading conditions and scratch tests. At the same time, a significant modification in surface properties of fluidized bed processed samples was detected by hardness measurement and X-ray diffraction analysis. In particular, the presence of compressive residual stresses and an increase of hardening level of external layers of samples were measured. An improvement of surface roughness was also achieved by fluidized bed processing, with Al_2O_3 film being able to cover the micro-peak and micro-valley topography produced by repeated impacts of Al_2O_3 powders onto aluminum substrates.

As a result of previous experimental findings, a considerable increase in the number of fatigue cycles to rupture for fluidized bed processed samples was observed. Accordingly, the improvements in fatigue strength resulted from *i)* superficial work hardening of fluidized bed processed substrates and *ii)* residual stresses. These phenomena caused retardation of crack initiation due respectively to large dislocation densities and retardation of micro-crack propagation due to surface compressive residual stress. A further enhancement of fatigue strength also resulted from improved surface topography, as seen in lower values of average roughness, slope and, particularly, in the maximum distance between peak and valley exhibited by Al_2O_3 coated surface. In this respect, a consistent number of cycles to fatigue failure according to loading conditions for fluidized bed processed and unprocessed material was measured, hence showing that, under different loading conditions, fluidized bed is able to induce improve-

ments in fatigue strength which measure even more than 25 times. Furthermore, very fast improvement of fatigue resistance of FB treated material according to processing time was measured, hence confirming the high degree of effectiveness of the technique developed.

Finally, it is worth noting that as the fluidized bed processing is a very low pressure process, it can be operated with basic equipment and without any particular precautions regarding operators safety and environmental impacts. What is more, fluidized bed apparatus can be scaled-up and fully automated at a moderate cost, thus making this technique a very good alternative to traditional systems.

References

[1] C.M. Verport, C. Gerdes, Metal Behavior and Surface Engineering, IITT-International, 1989, p. 1.
[2] B. Syren, H. Wohlfart, E. Macherauch, Arch. Eisenhuttenwes. 8 (1977) 421.
[3] F. Reidenbach, ASM Handbook, 10th edition, Surface Engineering, vol. 05, ASM International, 1994.
[4] T.S. Eriksson, A. Hjortsberg, G.A. Niklasson, C.G. Granqvist, Appl. Opt. 20 (1981).
[5] CERAC Incorporated, Tech. Publ. (2004).
[6] G.R. Leverant, B.S. Langer, A. Yuen, S.N. Hopkins, Met. Trans. A 10A (1979) 251.
[7] P. Muller, C.V. Verport, G.H. Gessinger, Proc. 1st Int. Conf. on Shot Peening, Paris, Sept. 14–17, 1981, p. 479.
[8] A.A. Mazhar, N. Ahmad, A.Q. Khan, Metal Behavior and Surface Engineering, IITT-International, 1989, p. 193.
[9] J.F. Davidson, R. Clift, D. Harrison, Fluidization, Academic Press, 1985.
[10] M. Barletta, V. Tagliaferri, Int. J. Mach. Tools Manuf. (2005) 1 (May).
[11] K.-H. Zum Gahr, Tribol. Int. (1998).
[12] M. Barletta, V. Tagliaferri, Int. J. Mat. Proc. Tech., July, submitted for publication.
[13] G.K. Williamson, R.A. Smallman, Phila. Mag. 1 (1956) 34.
[14] H. Wohlfart, ICSP 2, 1984 May.
[15] H.E. Franz, A. Olbricht, ICSP 3, 1987 October.
[16] R. Montanari, A. Sili, G. Costanza, Compos. Sci. Technol. 61 (2001) 2047.
[17] G. Costanza, R. Montanari, A. Sili, in: IJMPT, vol. 17, 2002, p. 214, nos ¾.
[18] K. Iida, T. Yamamoto, Metal Behavior and Surface Engineering, IITT-International, 1989, p. 323.
[19] B. Scholtes, Adv. Surf. Treat. 4 (1987) 59.